

Study of Microstructure and Mechanical properties of aluminum alloy welded by MIG and TIG welding processes

Veer Singh¹ Vikash Paroothi²

¹Assistant Professor, Department of Mechanical Engineering, Rama University, Kanpur
Veer2kz@gmail.com

²Assistant Professor, Department of Mechanical Engineering, MITRC, Alwar (Rajasthan)
vikas97d@gmail.com

Abstract— In this study, conventional fusion welding processes: MIG, TIG and solid state process friction stir welding (FSW) were applied to 6 mm thick plates of aluminium alloy. The weldments were evaluated by performing microstructural examinations including optical microscope and scanning electron microscope (SEM) and as well as hardness measurements. Mechanical testing has been done by means of tensile and bend tests. The mechanical properties and microstructural features of Aluminum (Al5052) weldments processed by gas tungsten arc welding (GTAW) and gas metal arc welding (GMAW) and friction stir welding are investigated. Weldments processed by both methods are mechanically softer than the parent material Al5052, and could be potential sites for plastic localization. The microstructure of the welds, including the nugget zone and heat affected zone, has been compared in these three methods using optical microscopy. The mechanical properties of the weld are have also been investigated using hardness and tensile tests. It is revealed that Al weldments processed by GTAW are mechanical more reliable than those by GMAW. The former bears higher strength, more ductility, and no apparent microstructure defects. Perceivable porosity in weldments by GMAW is found, which could account for the distinct mechanical properties between weldments processed by GTAW and GMAW. It is suggested that caution should be exercised when using GMAW for Al5052 in the

high-speed-train industry where such light weight metal is broadly used. However FSWed samples have more strength than that of MIG welded samples. The weld metal microstructure of MIG welded specimen contains equiaxed dendrites as a result of solidification process during MIG welding while FSWed specimen have wrought microstructure.

Keywords—Tungsten inert gas welding; metal inert gas welding; friction stir welding; aluminium alloy5052;mechanical properties; microstructures.

1. INTRODUCTION

Among aluminium alloys, 5086-H32 (AlMg4), commonly used in defence, shipbuilding, automotive, railway, aviation and aerospace industries, is a representative non-age-hardenable Al-Mg alloy that possesses an attractive combination of properties such as light weight, moderate high strength, good corrosion resistance, workability, and proven weldability, good electrical and thermal conductivity [1–6].

For the joining of aluminium alloys, fusion welding processes have commonly been used in several industrial applications. A solid state process-friction stir welding, (FSW) invented and patented at The Welding Institute (TWI) of UK in 1991, is considered to be the most significant development in metal joining in a decade. This relatively new welding process has initially and particularly been applied for welding the high strength aluminium alloys and other metallic alloys that are hard to weld by conventional fusion welding. FSW of aluminium alloys has been used in

the applications of aircraft, shipbuilding, automotive, railway, defense industries and

Table 1. Chemical composition and mechanical properties of base metal

Chemical composition (wt%)										
Si	Fe	Cu	Mn	Mg	Cr	Ni	Zn	V	Ti	Al
0.163	0.399	0.010	0.093	2.217	0.213	0.01	0.010	0.02	0.02	BAL
Mechanical properties										
Proof stress 0.2 (MPa)				Tensile strength (MPa)				Elongation (%)		
240				331				15.2		

attracted extensive research interest due to the potential engineering importance and problems such as reduced strength of the joints, distortions, residual stresses, gas porosities, metallurgical precipitations in the weld metal and HAZ, lack of fusion, high coefficient of thermal expansion, solidification shrinkage, high solubility of hydrogen and other gases associated with conventional welding [2–10].

The rapid development of FSW in aluminium alloys and its successful implementation into commercial applications has motivated its application to more non-ferrous materials and other metals [2, 9]. In FSW, as a basis, a non-consumable tool with a special designed pin and a shoulder is plunged into the abutting edges of the plates to be joined to a preset depth and moved along the weld joint. Heat is generated through the frictional contact between the rotating tool shoulder, abutting material surface and plastic deformation of work piece [2, 5, 6, 9, 11–14].

In the literature, friction stir weldability of 5083 aluminium alloy has been investigated by several researchers [8, 14–23]. However, a study about the friction stir weldability of 5052 B209 alloy has not been found up to now. It is not only important to show the feasibility of FSW, but also to delineate its advantages and/or disadvantages over other techniques [9]. So, the objective of this investigation is to determine and compare the microstructural and mechanical properties of double-sided friction stir (FS) welds and conventional MIG and TIG welds of 6mm thick 5052-B209 aluminium alloy. The microstructural investigation of the weld zones includes light optical microscope (LOM) and transmission electron microscope (TEM) examinations, EDX

analysis as well as hardness measurements with 200 g load. Mechanical testing, tensile and bend tests were applied and in addition, fracture surfaces of the joints were studied and discussed with microstructure and SEM images.

2. Material and experimental procedures

In this paper, a non-heat treatable 5052-B209 Al- -Mg alloy which is mainly used in the construction of tactical military vehicles and shipbuilding has been used. In Table 1, the chemical composition and the mechanical properties of the base metal have been demonstrated.

Welding processes that have been applied to the base metal are: MIG and TIG as conventional fusion welding processes and friction stir welding as solid state welding process. Butt joints of double sided welds were obtained.

MIG and TIG welds were produced semi-automatically in industrial conditions, with an ER 5356 (AlMg5Cr (A)) wire of 1.6 mm diameter in combination with 99.999 % Argon shield gas. Arc voltage and welding current varied respectively between 240 V and 300V and between 180 A and 200 A. I grooves were cleaned with acetone and stainless steel brush prior to welding. AISI 4340 (0.40 % C, 0.70 % Mn, 0.30 % Si, 0.80 % Cr, 1.80 % Ni, 0.25 % Mo) tool was used for friction stir welding of the plates shown in fig 1. M5 threaded tool had a shoulder diameter of 20 mm and 3.6 mm height standard pin. The welding tool was rotated in anti-clock direction with 2° tool tilting from the plate normal. 1600 rpm and 125 mm min⁻¹ tool rotational and translation speeds were used, respectively.

Visual inspection of the welds was made with reference to ANSI/AWS B.1.11. Weld

reinforcement and spatter dimensions were measured. All welded plates were subjected to distortion measurements.

As metallographic examination, the cross sections of the welded joints were prepared, polished and etched with modified Keller's reagent for about 30sec, visualized as macro- and micrographs using LOM.

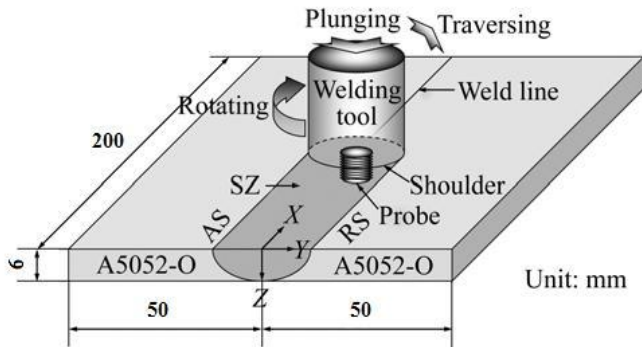


Fig.1 Schematic representation of friction stir welding process

SEM investigation has also been applied to the Thermo-mechanical affected zones of friction stir welded specimen. Vickers Micro hardness measurements were carried out as line analysis, under 200 g test load at 2 mm depth from the face and root side of each cross section of the welds.

For mechanical testing, transverse tensile (fig 3) and bend test specimens were prepared from the welded plates with reference to EN 895 and EN 910 standards, respectively.



Fig.2 Tinioulesen universal testing machine

Weld reinforcement of the specimens was ground off. The tests were carried out using a Tinioulesen universal testing machine (fig 2) at room temperature. To determine the fracture mode of welded joints, fracture surfaces of the specimens were examined using light microscope and scanning electron microscope (SEM).

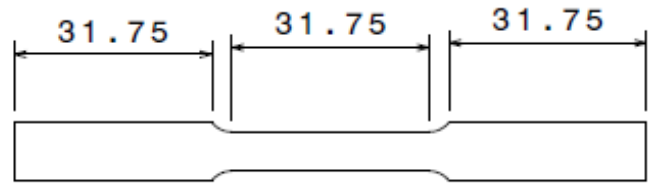


Fig.3 Tensile test specimen

3. Results and discussion

3.1. Sample preparation and microstructure examination

The samples were taken from butt welded pieces of Al5052 being the base metal. Pre-weld cleaning of weld joint surfaces was performed, in order to remove grease, rust, moisture in 20–30 mm distance of the groove on both sides. To examine the microstructures around the weldments, we prepared samples by cutting off a weldments in the transverse direction and ground with emery paper of finer grade (180, 320, 600, 800 and 1000) and polished using the 6 μ , 3 μ and 1 μ of diamond particles. The samples were etched with chemical solution that contained 150 ml distilled water, 6ml nitric acid, 3ml hydrofluoric acid (KELLER'S reagent) for about 20 seconds before being observed under the optical microscope (20x, 50x and 200x magnification) and also used to identify grain size and porosity in the weldments.

Scanning electron microscope (SEM) was also used to identify grain size and porosity in the weldments.

After the visual inspection of the plates, MIG and TIG welded joints were determined to be acceptable as no surface cracks and discontinuities were detected. Due to the high heat input, the largest amount of distortion was determined on the MIG welded plate.

The microstructural investigation was carried out on the metallographic

specimens of the joints using LOM, adapted with image analyses system. Micrographs of fusion and

friction stir welded samples are illustrated in Fig. 4. In fusion welded cross sections, depending on the

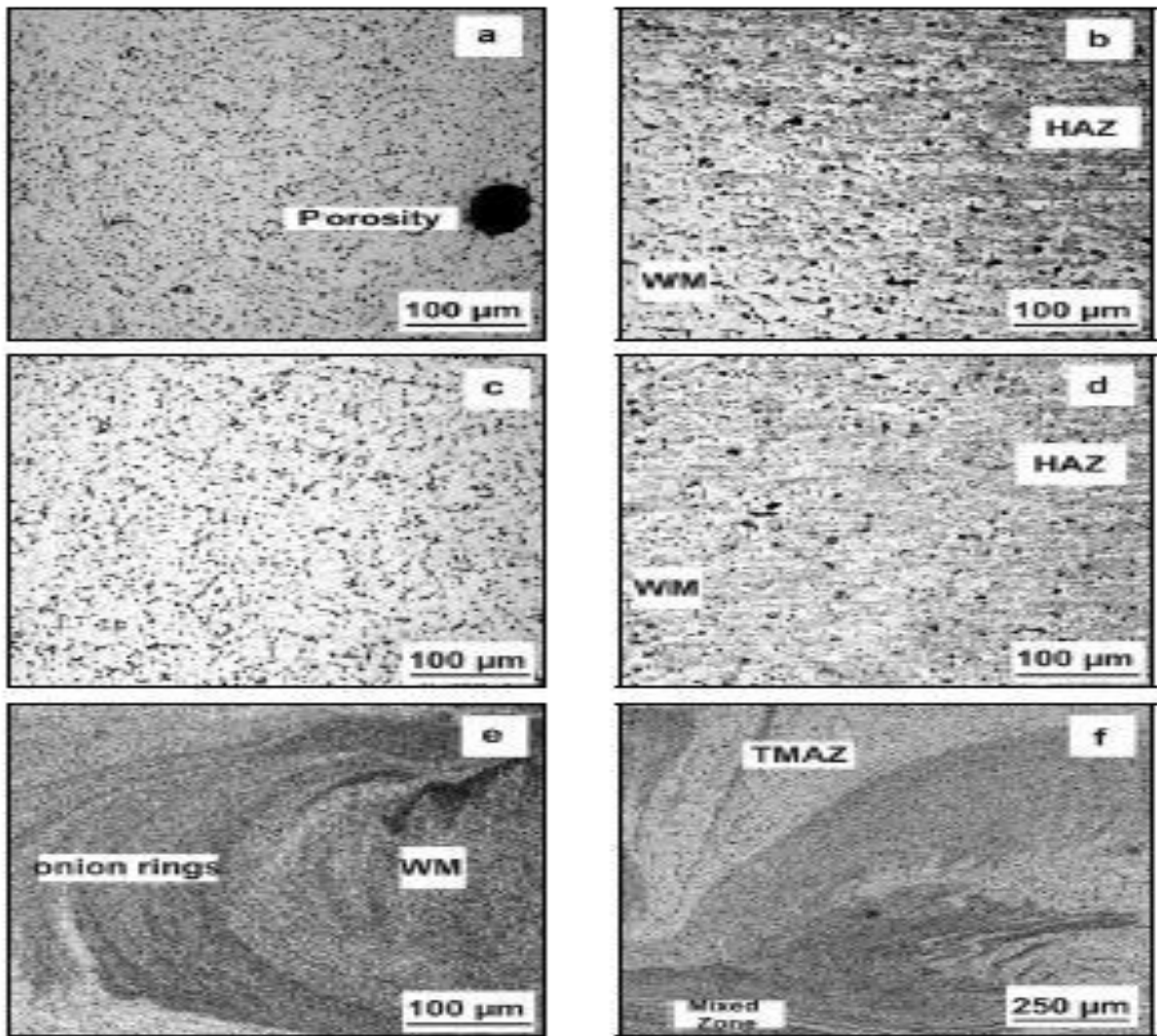


Fig.4 Micrographs of the weld zones:(a) MIG weld metal(WM),(b) MIG WM+HAZ,(c) TIG WM,(d) TIG welded WM+HAZ, (e) FS WM,(f) FS WM+ TMAZ.

fusion of the aluminium alloy and high temperatures experienced by adjacent material, a fairly wide heat affected zone (HAZ) has been observed.

As the same filler metal has been used for the MIG and TIG welding, similar microstructural morphologies have been observed, however some porosity has been determined in the weld metal (WM) of MIG welded sample. Based on the

microstructural characterization, three distinct zones have been observed in friction stir welded samples. The nugget zone with onion ring structure and thermo-mechanical affected zone (TMAZ) that experiences both temperature and deformation during the process and HAZ, have been identified. An onion ring structure can be observed in the nugget zone whose recrystallized fine grain

structure is generated as a result of plastic deformation and frictional heating. The nugget with onion rings and with a structure like pan-cake, the transition between the nugget and TMAZ, can be

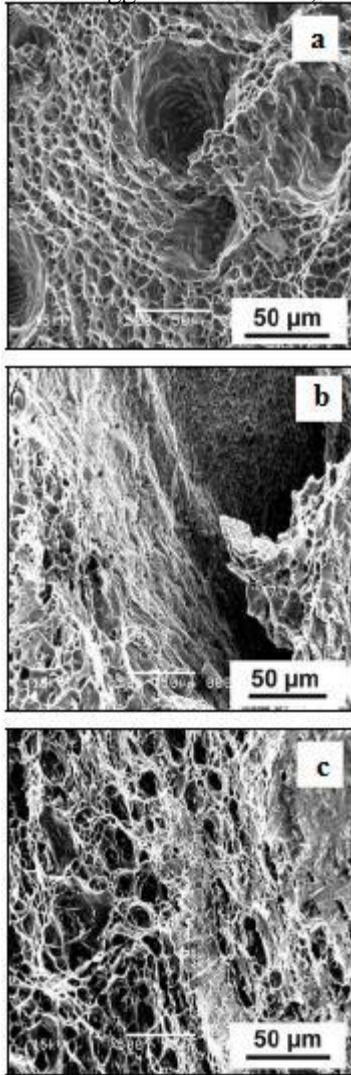


Fig.5 (a), (b), (c) SEM images of MIG, TIG and FS welded joints

Figure 5a is an enlarged SEM photograph showing a dimple pattern that indicates ductile fracture and the porosity in this matrix occurred. Figure 5b also contains the photograph of dimple patterns and some defects which caused fracture to initiate. Figure 5c exhibits the ductile fracture phenomena of FS welded specimens. Tensile testing of these joints showed that cracking tended to occur initially at the upper region of the joint and

observed at the friction stir welded 5086-H32 alloy as shown in Figs. 4e and 4f.

Propagated towards the bottom region. For the hardness distribution in the weld zones, the solid solution hardened Al alloys have shown very different behaviour than the precipitation hardening alloys as reported by Mishra and Ma [9] and Lee et al. [24]. In the papers, for precipitation hardening alloys, it is explained that a softened region was formed in the weld zone because the precipitates disappeared or coarsened by the welding heat. Especially, such a softening was caused by dissolution and growth of strengthening precipitates (Mg_2Si , $MgZn_2$) during the thermal cycle of the welding. However, for the solid solution hardened alloys, generally a roughly homogeneous was determined as hardness profile depending on the dislocation density and strain hardening mechanism of the alloys.

3.2. Hardness properties

The hardness profile of friction stir welded 5052-B209 sample has been determined almost homogeneous similar to the reported graphs in the literature for the 5083 alloy. It has been explained by Lee et al. [24], Svensson et al. [25] and Sato et al. [26–28], that this situation was mainly governed by not only dislocation density, but also the distribution and size of the small $Al_6(Mn, Fe)$ particles. Figure 6b shows the mean values of the tensile properties of MIG, TIG and friction stir welded joints. Examination of the tensile test results of the welded joints has demonstrated that the average joint efficiency values of the welded joints are 82 %, 76 % and 85 % of the base material, respectively.

The hardness plots confirm the order of the tensile strength values of the welded joints. Fracture of the welds occurred in the weld metal (WM) for fusion welded and thermo mechanically affected zone (TMAZ) advancing side for the friction stir welded joints, respectively. The strength increasing effect of strain hardened 5052-B209 aluminium alloy was eliminated by the high heat input of

fusion welding and porosities in weld metal are the reason. It was mentioned previously that the base material is in an extremely work hardened state. The base material has a Vickers hardness of about

130HV, very high for an alloy of this type. The hardness of FSWed samples is related to the hardness of the stir zone, whereas the hardness of MIG samples is related to the weld metal.

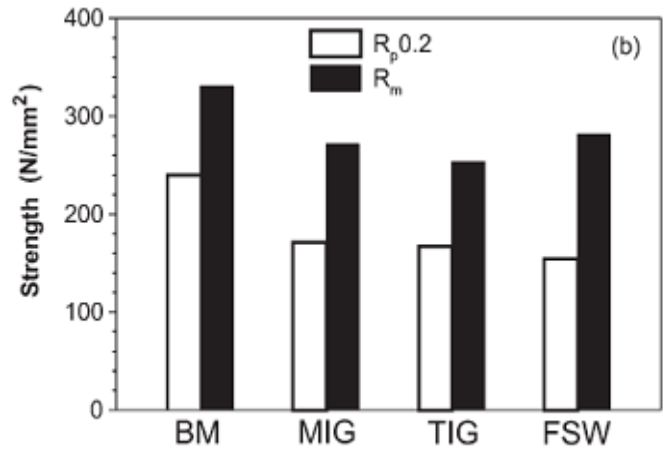
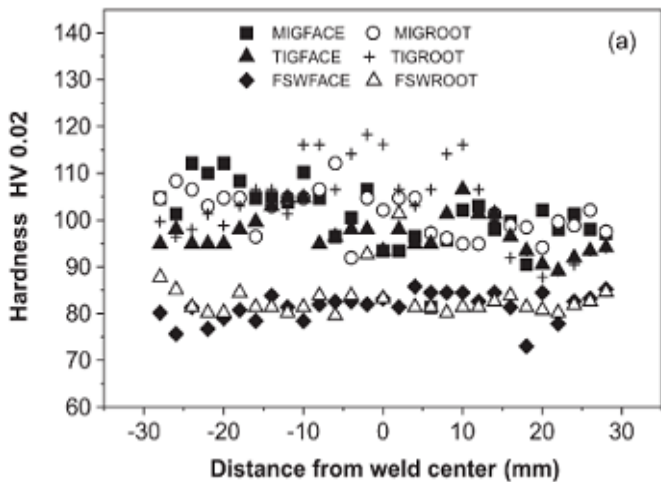


Fig.6 (a) First and second pass hardness distributions of MIG,TIG and FS welded joints, respectively,(b) Comparison of mean the base metal strength values with welded joints

Table.2 Summary of welding conditions applied for both GMAW and GTAW

Specification	GMAW	GTAW
Preheating	No	No
Welding current	Alternating current	Alternating current
Welding voltage	240v	240v
Shielding gas	100% argon	100% argon
Shielding gases flow rate	$2.5-3 \times 10^{-4} \text{ m}^3/\text{s}$	$2.5-3 \times 10^{-4} \text{ m}^3/\text{s}$
Post heating	No	No
Filler rod	ER5356	ER5356
Welding electrode	Aluminium rod coated with copper	Aluminium electrode

The Vicker micro-hardness of 5083 aluminum alloy is about $79.83 \pm 1.67 \text{ HV1}$, and those

in the GTAW and GMAW weldments are $79.38 \pm 1.89 \text{ HV1}$ and $72.15 \pm 5.18 \text{ HV1}$, respectively. Vickers micro-hardness of the GTAW weldments is almost the same as that of the parent material, while that in the GMAW weldments is about 10% less than that of the parent material. The variations in hardness mentioned above can be readily correlated with the microstructure developed both during and after the welding process. As stated above, the 5xxx series alloys are predominantly workhardenable alloys and so it is this microstructure, typical of rolling/work hardening that is the main contributor to the high hardness of this region compared to the weld zone (Kristensen *et al.* 2004; Uyyuru & Kailas 2006). It was shown that the welding process has dramatically altered the microstructure of the material in this region. The heavily worked microstructure of the base material has been completely replaced by equiaxed grains around $8 \mu\text{m}$ in diameter that have little sub-structure, typical of a recrystallized microstructure

and similar to that found previously in 5xxx, 6xxx and 7xxx series aluminum stir welds.

3.3. Tensile properties

The welded samples were tested for tensile strength using the Tinioulesen UTM. The edges of

Specimen	Tensile stress(MPa)	Elongation (%)
Double Vee-butt TIG welded specimen 1	100	2.86
Double Vee-butt TIG welded specimen 2	120	4.44
Double Vee-butt MIG welded specimen 1	150	4.88
Double Vee-butt MIG welded specimen 2	185	7.15
FSW tensile Specimen(1000 r/min)	204	21

The mechanical responses of both the parent materials and the welding zones are shown in fig 7. (a) gives the quasi-static uniaxial compressive stress-strain curves for the parent material, TAW and GMAW weldments shown in table 3. Here the ends represent the interruption of the tests at those points because there was no failure observed till the applied strain during compression. The quasistatic uniaxial tensile stress-strain behavior of GMAW and GTAW samples are shown. There is a striking difference in the ductility of the two types of

the test samples were fitted into the jaws of the testing machine and subjected to tensile stress until the sample fractured. During the test, the various stress-strain diagrams were drawn for each of the tensile stress until the sample fractured. During the test, the various stress-strain diagrams were drawn for each of the samples from where the tensile load is determined. This is used in determining the strength and stiffness of the materials.

Table 3. Tensile test results for welded specimens

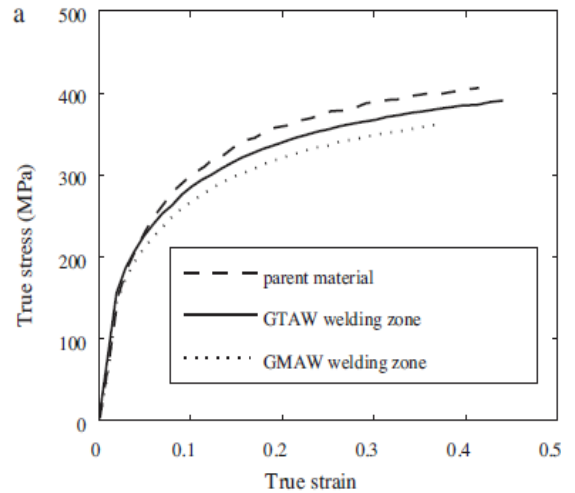


Fig.7 (a) compressive stress-strain (true) curve of parent material AL 5052, GTAW, GMAW weldments

weldments, by looking at the fracture points from the tensile stress-strain curves. Failure occurs in the weldments for both types of samples. From the macroscopic observations on the broken surfaces of the GMAW and GTAW welded samples, GTAW exhibits a ductile shear fracture in the whole fracture surface with a shear angle of 47°, while the GMAW one exhibits a fibrous fracture surface at one side and a shear fracture surface at another. They both have a gray, fibrous appearance. The dimples formed during the coalescence of micro voids suggest fracture in ductile manner. Fracture surfaces in GTAW welded samples have knife edged conical dimples, while dimple edges in the fracture surface

of GMAW samples are smooth ellipses. These differences indicate more plastic deformation in GTAW samples than that in GMAW samples. In the face and root bend test results of the welded specimens, although MIG and TIG welded specimens show some cracks, no crack was observed in friction stir welded specimens, see Table 4.

Mechanical testing by means of tensile and bend tests has proved some more advantages of the friction stir welding process compared to fusion welding processes. Selecting the best filler alloy for a given application depends on the desired performance relative to weldability, strength, ductility, and corrosion resistance. In general, the filler alloy selected should be similar in composition to the base metal alloy. Similarly, 5xxx filler alloys are used to join 5xxx-series base metal alloys. An exception to this rule is encountered when weldability becomes an issue.

Others Problems are with hot cracking encountered when welding under highly constrained conditions or when welding certain alloys that are highly susceptible to cracking. Such is the case when welding the alloys that have low range magnesium content. To avoid cracking, use of a high-magnesium filler alloy is recommended.

Table.4 bend test results of the MIG, TIG and FS welded joints

Welding process	Test type	Specimen code	Test result
MIG	Face bend	M86F1	No crack
TIG	Face bend	T86F1	Harmless crack
FSW	Face bend	F86F1	No crack

4. Conclusions

The conventional MIG and TIG welding processes and innovative friction stir welding (FSW) processes were successfully applied to join 5052-B209 aluminium alloy from double sides as it can be called as double-pass. The microstructural

properties and hardness distributions, mechanical properties, examining of fracture surfaces of the joints have been studied in the present work. Following conclusions can be drawn: The microstructure of double stir zones was mainly composed of onion ring structures in the nugget zones with fine and equiaxed grains, and double TMAZ were observed because of welding from double sides that improves the mechanical properties. In addition, the onion ring structure region becomes wider, as the tool rotation speed is increased.

The hardness profile was found roughly homogeneous similar to the examples in the literature. The present study has demonstrated that the tensile properties of FSW joints were more satisfactory than fusion welded joints. All fracture of FS welded specimens were occurred in TMAZ. Bend tests of welded plates have shown that FS welded specimens do not include any defect like fusion welded specimens. LOM and SEM examinations of the fracture surfaces exhibited porosities in MIG and TIG welds that have caused strength values to decrease; however FS welds do not include weld defects. And also the tensile strength of the FSWed plates is similar to that of the base metal (about 204MPa) and elongation is lower than that of the base metal.

Acknowledgements

The authors would like to acknowledge KS engineering works, for their contribution and technical support. The cooperation of Chennai CNC centre for making tensile test specimen using wire cut EDM is also acknowledged. In addition many thanks to Prof. N.Srirangarajalu and his team for SEM and optical photographs.

References

1. ZHOU, C.—YANG, X.—LUANET, G.: Scripta Materialia,53, 2005, p. 1187.

2. MATHERS, G.: *The Welding of Aluminium and Its Alloys*. Cambridge, Woodhead Publishing Limited 2002.
 3. ANDERSON, T.: *Welding Journal*, 81, 2002, p. 77.
 4. ANDERSON, T.: *Welding Journal*, 83, 2004, p. 28.
 5. JOHNSEN, M. R.: *Welding Journal*, 78, 1999, p. 35.
 6. KALLEE, S. W.—DA VENPORT, J.—NICHOLAS, E. D.: *Welding Journal*, 81, 2002, p. 47.
 7. TABAN, E.—KALUC, E.: *Kovove Mater.*, 44, 1, 2006, p. 25.
 8. KALUC, E.—TABAN, E.: *DVS Annual Welding Conference, Schweissen und Schneiden*, Essen, Germany 2005, p. 489.
 9. MISHRA, R. S.—MA, Z. Y.: *Materials Science and Engineering R*, 50, 2005, p. 1.
 10. DAWES, C. J.—THOMAS, W. M.: *Welding Journal*, 75, 1996, p. 41.
 11. CANTIN, G. M. D. et al.: *Science and Technology of Welding and Joining*, 10, 2005, p. 268.
 12. DAWES, C. J.—THOMAS, W.: *TWI Bulletin* 6, Reprint 493/6/95, Cambridge 1995, p. 124.
 13. COLLIGAN, K. J.—KONKOL, P. J.—FISHER, J.J.—PICKENS, J. R.: *Welding Journal*, 82, 2003, p.34.
 14. THREADGILL, P.: *TWI Bulletin*, Reprint 513/2/97, Cambridge 1997.
 15. PEEL, M.—STEUWER, A.—FREUSS, M.—WITHERS, P. J.: *Acta Materialia*, 51, 2003, p. 4791.
 16. JAMES, M. N.—HATTINGH, D. G.—BRADLEY, G.R.: *International Journal of Fatigue*, 25, 2003, p. 1389.
 17. LARSSON, H.—KARLSSON, L.: *Svetsaren*, 2, 2000, p. 6.
 18. LIU, H. J.—FUJII, H.—MAEDA, M.—NOGI, K.: *Transactions of Nonferrous Metals Society of China*, 13, 2003, p. 14.
 19. DICKERSON, T. L.—PRZYDATEK, J.: *International Journal of Fatigue*, 25, 2003, p. 1399.
 20. SHIGEMATSU, I.—KWON, Y. J.—SUZUKI, K.—IMAI, T.—SAITO, N.: *Journal of Materials Science Letters*, 22, 2003, p. 353.
 21. VAZE, S. P.—XU, J.—RITTER, R. J.—COLLIGAN, K. J.—FISHER, J. J.—PICKENS, J. R.: *Materials Science Forum*, 426–432, 2003, p. 2979.
 22. REYNOLDS, A. P.—LOCKWOOD, W. D.—SEIDAL, T. U.: *Materials Science Forum*, 331–337, 2000, p. 1719.
 23. MCLEAN, A. A.—POWELL, G. L. F.—BROWN, I.H.—LINTON, V. M.: *Science and Technology of Welding and Joining*, 8, 2003, p. 462.
 24. LEE, W. B.—YEON, Y. M.—JUNG, S. B.: *Materials and Engineering*, A355, 2003, p. 154.
 25. SVENSSON, L. E.—KARLSSON, L.—LARSSON, H.—KARLSSON, B.—FAZZINI, M.—KARLSSON, J.: *Science and Technology of Welding and Joining*, 5, 2000, p. 285.
 26. SATO, Y. S.—KOKOWA, H.—ENOMOTO, M.—JORGAN, S.: *Metall. Mater. Trans.*, A 30, 1999, p.2429.
 27. SATO, Y. S.—KOKOWA, H.—ENOMOTO, M.—JORGAN, S.—HASHIMOTO, J.: *Metall. Mater. Trans.*, A 30, 1999, p. 3125.
 28. SATO, Y. S.—PARK, S. H. C.—KOKOWA, H.: *Metall. Mater. Trans.*, A 32, 2001, p. 3033.
 29. TABAN, E.: *Investigation on Mechanical and Microstructural Properties of TIG, MIG and FS Welded 5xxx Series Aluminium Alloys*. [MSc Thesis]. Kocaeli University, Turkey 2004.
-